Indian J Pure Appl Math (2026) 57:1503–1520
https://doi.org/10.1007/s13226-024-00722-0

ORIGINAL RESEARCH

Uniformly convergent numerical method for two parameter singularly perturbed parabolic differential equations with discontinuous initial condition

Neha Kumari · S. Gowrisankar

Received: 5 October 2023 / Accepted: 12 November 2024 / Published online: 4 December 2024

Abstract This paper investigates a class of singularly perturbed problems with two small parameters having a jump discontinuity in the initial condition. To elucidate the nature of the singularity stemming from this discontinuity, a specific singular function is identified. By subtracting this singular function from the solution of the problem, a remainder function is obtained. This remainder function is then numerically estimated using an appropriate piece-wise uniform mesh, taking into consideration the relation between the two perturbation parameters. Through rigorous error analysis, the numerical scheme employed is demonstrated to be parameter-uniform. The numerical results obtained in this research align well with the theoretical point-wise error bounds, affirming the robustness and accuracy of the proposed method.

Keywords Singularly perturbed · Two parameter · Discontinuous initial condition · Piece-wise uniform mesh · Interior layer

Mathematics Subject Classification 65M06 · 65M15 · CR G1.8

1 Introduction

The development of singular perturbation problems is the result of modeling real world problems. The convective heat transfer problems with large Peclet number and the Navier–Stokes equations in fluid dynamics with large Reynolds number, are the finest examples to use. Depending upon the number of perturbation parameters, the continuity or discontinuity of the convective coefficient, the source function or initial and/or boundary conditions throughout the whole domain under consideration, singular perturbation problems may be divided into many types. The two highest-order derivatives of these problems are multiplied by the perturbation parameters, i.e., ε is multiplied to diffusion term and μ is multiplied to the convection term, to create two-parameter singularly perturbed problems (TP-SPPs). Numerous real-world applications of TP-SPPs may be found in fields like lubrication theory, the field transport phenomena in chemistry, flow through unsaturated porous media and chemical flow reactor theory [19], to name just a few. The solutions to singularly perturbed problems exhibits an abrupt change in the boundary layer region(s), whereas the surrounding region exhibits normal behavior. The numerical treatment of singularly perturbed differential equations is very computationally challenging because

Communicated by G.D. Veerappa Gowda.

N. Kumari · S. Gowrisankar (✉)
Department of Mathematics, National Institute of Technology Patna, Patna 800005, India
E-mail: s.gowri@nitp.ac.in

N. Kumari
E-mail: nehak.ph21.ma@nitp.ac.in

of the relatively small perturbation parameter value and the existence of boundary and/or interior layers. For more discussions on the behavior of layers, the readers are referred to [3,15,16,21].

This paper aims to examine the the following problem class: find u such that

$$\begin{cases} \mathcal{L}u := \frac{\partial u}{\partial t} - \varepsilon \frac{\partial^2 u}{\partial x^2} + \mu b(t) \frac{\partial u}{\partial x} + c(t)u = g(x,t), \ (x,t) \in G := (0,1) \times (0,T], \\ u(x,t) = \chi(x) \text{ on } \Omega_b, \ [\chi](p) \neq 0, \ 0 < p = O(1) < 1, \\ u(x,t) = 0 \text{ on } \Omega_l \cup \Omega_r, \end{cases} \tag{1}$$

where $0 < \varepsilon, \ \mu < 1$ are the two perturbation parameters, $\Omega_l = \{(0,t)|0 < t \leq T\}, \ \Omega_r = \{(1,t)|0 < t \leq T\}$ and $\Omega_b = \{(x,0)|0 < x < 1\}$. We suppose that $b(t) \geq \beta > 0, \ c(t) \geq \gamma > 0; \ b, \ c, \ g \in C^{4+k}(\overline{G})$[1] The compatibility conditions,

$$\chi \in C^4((0,1)/\{p\}); \quad \chi^{(i)}(0) = \chi^{(i)}(1) = 0; \ 0 \leq i \leq 4,$$

near the end points $(0,0)$ and $(1,0)$ ensures that no classical singularity appears near these corner points. To solve these kind of problems, adaptable numerical techniques must be created whose accuracy is independent of the perturbation parameter(s) and whose singularity can be clearly identified.

The study of one-parameter singular perturbation problems has a long history, but recent years have seen a growing focus on developing robust methods for solving two-parameter singular perturbation problems (TP-SPPs). To the best of our knowledge, O'Malley [17–19] was the first to delve deeply into the asymptotic behavior of TP-SPPs, highlighting the critical role of the ratio between μ^2 and ε. In 2001, Vulanović [26] explored finite difference methods when $\mu = \varepsilon^{\frac{1}{2}+\lambda}$ $(\lambda > 0)$ on layer-adapted meshes. In 2003, Roos and Uzelac [22] used the SDFEM method achieving almost second-order convergence. Using an upwind finite difference operator on a piecewise uniform mesh, Linß and Roos [14] demonstrated first-order convergence in 2004. A second order numerical method employing the central difference, upwind, and mid-point methods was proposed in 2006 by Gracia et al. [5]. For time-dependent TP-SPPs, a parameter-uniform numerical method was proposed by O'Riordan et al. [20] in 2006. He employed the upwind finite difference operator and demonstrated first order convergence in both space and time. In 2008, Kadalbajoo and Yadaw [11] presented a numerical method based on B-spline collocation on a Shishkin mesh and acheived an almost second-order convergence. In 2014, Zahra et al. [27] introduced a spline-based technique achieving second-order convergence in space and first-order convergence in time. In 2015, Jha and Kadalbajoo [10] developed a finite difference method using a Bakhvalov-Shishkin type mesh demonstrating first-order convergence in both time and space. Das and Mehramann [2] proposed a uniformly convergent method showcasing first-order convergence in both spatial and temporal directions in 2016. In 2019, Gupta et al. [8] demonstrated nearly second-order accuracy in space and first-order accuracy in time by using a hybrid difference scheme on a Shishkin mesh for space and an Euler backward difference scheme for time. In 2020, Singh and Natesan [25] employed the NIPG method on various layer-adapted grids. On an exponentially graded mesh, Shivhare et al. [24] proposed a quadratic B-spline collocation method in 2021, achieving second-order uniform convergence. Although many numerical techniques have been developed for TP-SPPs with smooth data, research on methods for non-smooth data is relatively limited, particularly when the intial condition is discontinuous.

So far, some research has been conducted for one parameter SPPs with discontinuous initial condition. In 1969, Bobisud [1] constructed asymptotic expansions for the solution involving the singularity which arises due to the discontinuous initial condition. In 1994, Hemkar and Shishkin [9] introduced a specially fitted scheme showcasing uniform convergence. In 2009, Shishkin [23] employed the Richardson scheme for the singularly perturbed parabolic reaction-diffusion equation in the case of a discontinuous initial condition. In 2020, Gracia and O'Riordan [6] dealt with reaction-diffusion problems with discontinuities in the initial and/or the boundary

[1] The space $C^{4+k}(D)$ is defined as,

$$C^{4+k}(D) = \left\{ z : \frac{\partial^{n+m} z}{\partial x^n \partial t^m} \in C^{0+k}(D), \ 0 \leq n + 2m \leq 4 \right\},$$

where the space $C^{0+k}(D)$ is defined as,

$$C^{0+k}(D) = \left\{ f \in D : \sup_{s_1 \neq s_2, \ s_1, s_2 \in D} \frac{|f(s_1) - f(s_2)|}{||s_1 - s_2||^k} \right\},$$

with respect to the metric $|| \cdot ||$ where $||s_1 - s_2||^2 = (p_1 - p_2)^2 + |q_1 - q_2| \ \forall s_i = (p_i, q_i) \in \mathbb{R}^2, \ i = 1, 2.$

data and in 2021, they [4,7] dealt with convection-diffusion problem with a discontinuous initial condition. For Two parameter SPPs with discontinuous initial condition, Kumari and Gowrisankar [12] employed a cubic B-spline collocation method in 2024. In this paper, we have extended these ideas to address a class of TP-SPPs with discontinuous initial data as described in Eq. (1).

An interior layer emerges from the point $(p, 0)$ because of the presence of discontinuity in the initial function $\chi(x)$ at $x = p \in (0, 1)$. To capture the singularity resulting from the discontinuous initial condition, a singular function, denoted below by $\mathcal{A}(x, t)$, is identified by following the same approach as in [1]. By subtracting this singular function from the solution of the problem, denoted as $u(x, t)$, we obtain a remainder function, $y(x, t)$ which is again a two-parameter singular perturbation problem, but with continuous initial data. Naturally, the analysis for the remainder function $y(x, t)$ splits into two cases: $\mu^2 \leq \frac{\zeta\varepsilon}{\beta}$ and $\mu^2 \geq \frac{\zeta\varepsilon}{\beta}$ where $\zeta = \min_{\overline{G}}\left\{\frac{c}{b}\right\}$. In the first case, the reduced problem is

$$c(t)y_0(x, t) + \frac{\partial y_0}{\partial t} = g(x, t), \text{ and } y_0(x, 0) = y(x, 0). \tag{2}$$

Therefore, in both neighborhoods of $x = 0$ and $x = 1$, boundary layers of width $O(\sqrt{\varepsilon})$ is predictable. However, in the second case, the reduced problem,

$$\begin{cases} \mu b(t)\frac{\partial y_\mu}{\partial x} + c(t)y_\mu(x, t) + \frac{\partial y_\mu}{\partial t} = g(x, t), \\ y_\mu(x, 0) = y(x, 0) \text{ and } y_\mu(0, t) = y(0, t), \end{cases} \tag{3}$$

is a one parameter singularly perturbed problem. Boundary layer of width $O(\mu)$ appears in the right neighbourhood of $x = 0$ and boundary layer of width $O\left(\frac{\varepsilon}{\mu}\right)$ appears in the left neighbourhood of $x = 1$. The path of the characteristic curve Ω, associated with the reduced problem, is implicitly defined by,

$$\Omega = \left\{(p(t), t) \mid p'(t) = \mu b(t),\ p(0) = p\right\}.$$

In this paper, we will solve the problem outlined in equation (1). For spatial discretization, we will employ the standard central differences and the backward Euler method on a piecewise uniform Shishkin mesh, while the implicit Euler method on a uniform mesh will be used for time discretization. The transition points are explicitly defined for this layer adapted mesh. The rigorous error analysis will demonstrate that the proposed numerical method achieves parameter-uniform convergence. Specifically, it will be shown that the method attains first-order convergence in both the temporal variable and the spatial variable. This ensures that the numerical solution remains accurate and stable, making it robust and reliable for solving TP-SSPs with discontinuous initial condition.

An overview of the contents of the paper is described as follows. In §2, the singular function $\mathcal{A}(x, t)$ is defined and the continuous problem is stated. In §3, we establish *a priori* bounds on $y(x, t)$ and its derivatives. Also, the decomposition of the solution in regular and singular components along with the bounds on the components is established. In §4, we construct a piece-wise uniform mesh for the space variable and provide a numerical scheme for the discrete problem. In §5, we shall construct error bound that is parameter-uniform on the numerical approximations. In §6, two test examples are provided to demonstrate the numerical scheme and also to back up the theoretical error bounds. In §7, some concluding remarks have been included.

Notation: Throughout this paper, the term C refers to a positive constant independent of ε, μ, N (number of mesh elements used in space direction) and M (number of mesh elements used in time direction). The L_∞ norm on the domain G is denoted by $||\cdot||_G$. The jump of the function $\chi(x)$ at the point $x = p$ is defined as $[\chi](p) = \chi(p^+) - \chi(p^-)$.

2 Continuous problem

Define the singular function $\mathcal{A}(x, t)$ as follows:

$$\mathcal{A}(x, t) = \frac{1}{2}\left(\sum_{r=0}^{4}[\chi^{(r)}](p)\frac{(-1)^r}{r!}\phi_r(x, t)\right)e^{-\int_0^t c(\theta)d\theta}.$$

The functions $\{\phi_r\}_{r=0}^{4}$ are defined in such a way that each ϕ_r is smooth in $G\backslash\Omega$, $L\phi_r = 0$; $\phi_r \in C^{r-1+k}(\overline{G})$, $r \geq 1$ and are given by,

$$\phi_0(x,t) := \text{erfc}\left(\frac{p(t)-x}{2\sqrt{\varepsilon t}}\right), \tag{4a}$$

$$\phi_1(x,t) := (p(t)-x)\phi_0 - 2\frac{\sqrt{\varepsilon t}}{\pi}\mathcal{K}, \tag{4b}$$

$$\phi_r(x,t) := (p(t)-x)\phi_{r-1} + 2\varepsilon t(r-1)\phi_{r-2},\ r = 2,3,4, \tag{4c}$$

where the two singular functions (see [1] and [7]) are described as follows:

$$\text{erfc}(\hat{z}) := \frac{2}{\sqrt{\pi}}\int_{z=\hat{z}}^{\infty} e^{-z^2}dz,\ \ \mathcal{K}(x,t) := e^{-\frac{(x-p(t))^2}{4\varepsilon t}}.$$

It is now possible to define the remainder function as follows:

$$y(x,t) = u(x,t) - \mathcal{A}(x,t). \tag{5}$$

Now, $y(x,t)$ satisfies the following problem:

$$\begin{cases} \mathcal{L}y = g(x,t),\ (x,t) \in G, \\ y(x,0) = \begin{cases} \chi(x), & x < p, \\ \chi(p^-), & x = p, \\ \chi(x) - \sum_{r=0}^{4}[\chi^{(r)}](p)\frac{(-1)^r(p-x)^r}{r!}, & x > p, \end{cases} \\ y(0,t) = -\mathcal{A}(0,t),\ 0 < t \leq T, \\ y(1,t) = -\mathcal{A}(1,t),\ 0 < t \leq T. \end{cases} \tag{6}$$

To ensure that there is no interaction between the interior layer and the boundary layers, a restriction on the final time T is introduced as follows: there exists $0 < \omega < 1$ such that $\omega := \frac{1-p(T)}{1-p}$. See [7] for more details.

3 Decomposition of the solution

We will now state a continuous maximum principle, whose proof is standard.

Lemma 3.1 *If $z \in C^2(G) \cap C^0(\overline{G})$ such that $\mathcal{L}z|_G \geq 0$ and $z|_{\partial G} \geq 0$, then $z|_{\overline{G}} \geq 0$.*

Lemma 3.2 *If $y(x,t)$ is the solution of the problem* (6)*, then the following bound hold:*

$$||y|| \leq \frac{T||g||}{\gamma} + ||y||_{\partial G}.$$

Proof See [12] for more details. □

We will now establish *a priori* bounds on the solution y of the problem (6) and its derivatives. In later sections, these bounds will be needed in order to properly conduct the error analysis.

Lemma 3.3 *The derivatives of the solution $y(x,t)$ of the problem* (6) *satisfy the following bound*

$$\left|\left|\frac{\partial^{n+m}y}{\partial x^n \partial t^m}\right|\right| \leq C\begin{cases} \frac{1}{(\sqrt{\varepsilon})^n}, & \mu^2 \leq \frac{\zeta\varepsilon}{\beta}, \\ (\frac{\mu}{\varepsilon})^n, & \mu^2 \geq \frac{\zeta\varepsilon}{\beta}, \end{cases} \tag{7}$$

where $n,\ m$ are any two non-negative integers such that $0 \leq n + 2m \leq 4$.

Proof The argument splits into two cases:

Case 1: When $\mu^2 \leq \frac{\zeta\varepsilon}{\beta}$.

Consider the transformation $\xi = \frac{x}{\sqrt{\varepsilon}}$. Under this transformation, the domain becomes $\tilde{G} = \left(0, \frac{1}{\sqrt{\varepsilon}}\right) \times (0, T]$. Additionally, we have $\tilde{y}(\xi, t) = y(x, t)$, with $\tilde{b}$, $\tilde{c}$, and $\tilde{f}$ defined in a similar manner. Applying this transformation to (6) results in:

$$-\tilde{y}_{\xi\xi} + \frac{\mu}{\sqrt{\varepsilon}}\tilde{b}\tilde{y}_{\xi} + \tilde{c}\tilde{y} + \tilde{y}_t = \tilde{g}, \text{ on } \tilde{G}.$$

Then for every $\delta \in \left(0, \frac{1}{\sqrt{\varepsilon}}\right)$ and $\kappa > 0$, let $R_{\delta,\kappa} = ((\delta - \kappa, \delta + \kappa) \times (0, T]) \cap \tilde{G}$. For each $(\delta, \kappa) \in \tilde{G}$, we use [13] to obtain the following bounds for $1 \leq n + 2m \leq 4$:

$$\left|\left|\frac{\partial^{n+m}\tilde{y}}{\partial\xi^n\partial t^m}\right|\right|_{\bar{R}_{\delta,\kappa}} \leq C \max\left\{||\tilde{y}||, \sum_{n+2m=0}^{2}\left|\left|\frac{\partial^{n+m}\tilde{g}}{\partial\xi^n\partial t^m}\right|\right|_{\bar{R}_{\delta,\kappa}}\right\},$$

where C is independent of the rectangle $R_{\delta,\kappa}$. Transforming back to the original (x, t) variables yields the desired result.

Case 2: When $\mu^2 \geq \frac{\zeta\varepsilon}{\beta}$.

Introduce the transformation $\upsilon = \frac{\mu x}{\varepsilon}$, $\tau = \frac{\mu^2 t}{\varepsilon}$. Applying this transformation to (6), we obtain for $\hat{y}(\upsilon, \tau) = y(x, t)$,

$$-\hat{y}_{\upsilon\upsilon} + \hat{b}\hat{y}_{\upsilon} + \frac{\varepsilon}{\mu^2}\hat{c}\hat{y} + \hat{y}_{\tau} = \frac{\varepsilon}{\mu^2}\hat{g}, \text{ on } \hat{G} = \left(0, \frac{\mu}{\varepsilon}\right) \times \left(0, \frac{\mu^2 T}{\varepsilon}\right].$$

Repeating the same argument as in the previous case gives us the desired result.

□

To obtain parameter uniform error estimates, the solution to (6) is decomposed into smooth and singular components as follows:

$$y(x, t) = v(x, t) + w_l(x, t) + w_r(x, t), \tag{8}$$

where $v(x, t)$, $w_l(x, t)$ and $w_r(x, t)$ are the smooth, left singular and right singular components of the solution, respectively. Also, these components satisfy the following differential equations:

$$\begin{aligned} &\mathcal{L}v = g, \ v(x, 0) = y(x, 0), \\ &v(0, t) \text{ and } v(1, t) \text{ are chosen suitably,} \end{aligned} \tag{9a}$$

$$\begin{aligned} &\mathcal{L}w_l = 0, \ w_l(x, 0) = w_l(1, t) = 0, \\ &w_l(0, t) = y(0, t) - v(0, t) - w_r(0, t), \end{aligned} \tag{9b}$$

$$\begin{aligned} &\mathcal{L}w_r = 0, \ w_r(x, 0) = 0, \\ &w_r(1, t) = y(1, t) - v(1, t), \ w_r(0, t) \text{ is chosen suitably.} \end{aligned} \tag{9c}$$

Theorem 3.4 *The smooth component $v(x, t)$ satisfy the following bounds,*

$$\left|\left|\frac{\partial^{n+m}v}{\partial x^n\partial t^m}\right|\right| \leq C \begin{cases} 1 + (\sqrt{\varepsilon})^{3-n}, & \mu^2 \leq \frac{\zeta\varepsilon}{\beta}, \\ 1 + (\frac{\mu}{\varepsilon})^{n-3}, & \mu^2 \geq \frac{\zeta\varepsilon}{\beta}, \end{cases} \tag{10}$$

for any two non-negative integers n, m such that $0 \leq n + 2m \leq 4$.

Proof The detailed proof follows from [8]. □

Lemma 3.5 *If the solution of* (6) *is decomposed as in* (8)*, then the singular components w_l and w_r satisfies the bounds given below:*

$$|w_l(x,t)| \le Ce^{-\rho_1 x},\ |w_r(x,t)| \le Ce^{-\rho_2(1-x)}, \tag{11a}$$

$$\text{where } \rho_1 = \begin{cases} \frac{\sqrt{\zeta\beta}}{2\sqrt{\varepsilon}}, & \mu^2 \le \frac{\zeta\varepsilon}{\beta}, \\ \frac{\zeta}{2\mu}, & \mu^2 \ge \frac{\zeta\varepsilon}{\beta}, \end{cases} \text{ and } \rho_2 = \begin{cases} \frac{\sqrt{\zeta\beta}}{2\sqrt{\varepsilon}}, & \mu^2 \le \frac{\zeta\varepsilon}{\beta}, \\ \frac{\mu\beta}{2\varepsilon}, & \mu^2 \ge \frac{\zeta\varepsilon}{\beta}. \end{cases} \tag{11b}$$

Proof Use the barrier functions

$$\xi_l^{\pm}(x,t) = Ce^{-\rho_1 x} \pm w_l(x,t),$$

and

$$\xi_r^{\pm}(x,t) = Ce^{-\rho_2(1-x)} \pm w_r(x,t),$$

to obtain the required bound on $|w_l(x,t)|$ and $|w_r(x,t)|$ respectively. □

The bounds on the singular components w_l and w_r when $\mu^2 \le \frac{\zeta\varepsilon}{\beta}$ follows from the Lemma 3.3. When $\mu^2 \ge \frac{\zeta\varepsilon}{\beta}$, the bounds on w_r follows from the Lemma 3.3 and the bounds on w_l are stated below.

Lemma 3.6 *When $\mu^2 \ge \frac{\zeta\varepsilon}{\beta}$, $w_l(x,t)$ satisfy the following bounds for all non-negative integers n, m such that $0 \le n+2m \le 4$:*

$$\left\| \frac{\partial^{n+m} w_l}{\partial x^n \partial t^m} \right\| \le \frac{C}{\mu^n}.$$

Proof Consider the following decomposition,

$$w_l(x,t) = w_0(x,t) + \varepsilon w_1(x,t) + \varepsilon^2 w_2(x,t) + \varepsilon^3 w_3(x,t), \tag{12}$$

where

$$\begin{aligned} &\mu b(t)\frac{\partial w_0}{\partial x} + c(t)w_0 + \frac{\partial w_0}{\partial t} = 0;\ w_0(x,0) = 0,\ w_0(1,t) = 0, \\ &\mu b(t)\frac{\partial w_1}{\partial x} + c(t)w_1 + \frac{\partial w_1}{\partial t} = \frac{\partial^2 w_0}{\partial x^2};\ w_1(x,0) = 0,\ w_1(1,t) = 0, \\ &\mu b(t)\frac{\partial w_2}{\partial x} + c(t)w_2 + \frac{\partial w_2}{\partial t} = \frac{\partial^2 w_1}{\partial x^2};\ w_2(x,0) = 0,\ w_2(1,t) = 0, \\ &\mathcal{L}w_3 = \frac{\partial^2 w_2}{\partial x^2};\ w_3(x,t) = 0, \forall (x,t) \in \partial G. \end{aligned}$$

By using proof-by-contradiction, we can easily establish the result given below by using the fact that $b(t) > 0$ and $c(t) > 0$.

$$\text{If } \mu b(t)\frac{\partial z}{\partial x} + c(t)z + \frac{\partial z}{\partial t} \ge 0 \text{ on G and } z \ge 0 \text{ on } \Omega_b \cup \Omega_r, \text{ then } z \ge 0 \text{ on } \overline{G}. \tag{13}$$

Using this argument and the arguments given in [20], we can easily obtain the following bounds for all non-negative integers n, m such that $0 \le n+2m \le 4$:

$$\left\| \frac{\partial^{n+m} w_0}{\partial x^n \partial t^m} \right\|_{\overline{G}} \le \frac{C}{\mu^n}. \tag{14}$$

Again, for $w_1(x,t)$ and $w_2(x,t)$, we have:

$$\left\| \frac{\partial^{n+m} w_1}{\partial x^n \partial t^m} \right\|_{\overline{G}} \le \frac{C}{\mu^{n+2}}, \quad \text{and} \quad \left\| \frac{\partial^{n+m} w_2}{\partial x^n \partial t^m} \right\|_{\overline{G}} \le \frac{C}{\mu^{n+4}}, \quad 0 \le n+2m \le 4. \tag{15}$$

For $w_3(x,t)$, we can easily get:

$$||w_3||_{\overline{G}} \le \frac{C}{\mu^6},$$

by using the Lemma 3.2 and bounds for $w_2(x,t)$. Finally, from Lemma 3.3, we obtain higher order derivatives of $w_3(x,t)$ for all non-negative integers n, m such that $0 \le n+2m \le 4$. Substituting these bounds in the equation (12) and using the inequality $\mu^2 \ge \frac{\zeta\varepsilon}{\beta}$, we get the desired bound. □

4 The discrete problem

The problem (6) is approximated using the standard central upwind scheme and backward Euler method on a mesh $\overline{G}^{N,M} = \{x_n\}_{n=0}^{N} \times \{t_m\}_{m=0}^{M}$ which incorporates a uniform mesh for the time variable t and a piece-wise uniform mesh for the space variable x. The mesh for the time variable is given by,

$$\{t_m = m\Delta t,\ m = 0, 1, ..., M\},$$

where $\Delta t = T/M$. The piece-wise uniform mesh for the space variable is defined with respect to the transition points,

$$\sigma_1 = \begin{cases} \min\left\{\frac{1}{4}, \frac{2\sqrt{\varepsilon}}{\sqrt{\zeta\beta}} ln\ N\right\}, & \mu^2 \le \frac{\zeta\varepsilon}{\beta}, \\ \min\left\{\frac{1}{4}, \frac{2\mu}{\zeta} ln\ N\right\}, & \mu^2 \ge \frac{\zeta\varepsilon}{\beta}, \end{cases} \text{ and } \sigma_2 = \begin{cases} \min\left\{\frac{1}{4}, \frac{2\sqrt{\varepsilon}}{\sqrt{\zeta\beta}} ln\ N\right\}, & \mu^2 \le \frac{\zeta\varepsilon}{\beta}, \\ \min\left\{\frac{1}{4}, \frac{2\varepsilon}{\mu\beta} ln\ N\right\}, & \mu^2 \ge \frac{\zeta\varepsilon}{\beta}, \end{cases} \tag{16}$$

which splits the interval $[0, 1]$ into three sub-intervals $[0, \sigma_1] \cup [\sigma_1, 1-\sigma_2] \cup [1-\sigma_2, 1]$ in the ratio $\frac{N}{4} : \frac{N}{2} : \frac{N}{4}$. More specifically,

$$x_n = \begin{cases} \frac{4\sigma_1 n}{N}, & 0 \le n \le \frac{N}{4}, \\ \sigma_1 + 2(1-\sigma_1-\sigma_2)\left(n - \frac{N}{4}\right), & \frac{N}{4} < n \le \frac{3N}{4}, \\ 1 - \sigma_2 + \left(n - \frac{3N}{4}\right)\frac{4\sigma_2}{N}, & \frac{3N}{4} < n \le N. \end{cases} \tag{17}$$

For $n = 1, 2, \ldots, N$, we set $h_n := x_n - x_{n-1}$. We denote by $\partial G^{N,M} := \overline{G}^{N,M}/G$.

The discrete problem is defined as follows: find $\mathcal{Y}$ such that

$$\begin{cases} \mathcal{L}^{N,M}\mathcal{Y} := D_t^-\mathcal{Y} - \varepsilon\delta_x^2\mathcal{Y} + \mu b D_x^-\mathcal{Y} + c\mathcal{Y} = g,\ t_m > 0 \\ \mathcal{Y}(x_n, t_m) = y(x_n, t_m),\ (x_n, t_m) \in \partial G^{N,M}. \end{cases} \tag{18}$$

The finite difference operators D_x^+, D_x^-, D_t^- and δ_x^2 are given by

$$D_x^+\mathcal{Y}_n^m = \frac{\mathcal{Y}_{n+1}^m - \mathcal{Y}_n^m}{h_{n+1}}, \quad D_x^-\mathcal{Y}_n^m = \frac{\mathcal{Y}_n^m - \mathcal{Y}_{n-1}^m}{h_n},$$
$$D_t^-\mathcal{Y}_n^m = \frac{\mathcal{Y}_n^m - \mathcal{Y}_n^{m-1}}{\Delta t}, \quad \text{and} \quad \delta_x^2\mathcal{Y}_n^m = \frac{D_x^+\mathcal{Y}_n^m - D_x^-\mathcal{Y}_n^m}{(h_n + h_{n+1})/2},$$

where $\mathcal{Y}_n^m = \mathcal{Y}(x_n, t_m)$.

For the finite difference operator in (18), we will now state a discrete maximum principle whose proof is standard.

Lemma 4.1 (Discrete maximum principle) *Let Z be any mesh function satisfying the following two criteria: (i)* $\mathcal{L}^{N,M}Z \ge 0$ *on* $G^{N,M}$*, and (ii)* $Z \ge 0$ *on* $\partial G^{N,M}$*, then* $Z \ge 0$ *on* $\overline{G}^{N,M}$.

The following lemma is a standard corollary to the above discrete maximum principle.

Lemma 4.2 *Let Z be any mesh function, then*

$$||Z|| \le C||\mathcal{L}^{N,M}Z|| + ||Z||_{\partial G^{N,M}}.$$

The discrete solution of the problem (18) can be decomposed as follows:

$$\mathcal{Y} = \mathcal{V} + \mathcal{W}_l + \mathcal{W}_r, \tag{19}$$

where

$$\mathcal{L}^{N,M}\mathcal{V} = \mathcal{L}v \text{ on } G^{N,M} \text{ and } \mathcal{V} = v \text{ on } \partial G^{N,M}, \tag{20a}$$

$$\mathcal{L}^{N,M}\mathcal{W}_l = 0 \text{ on } G^{N,M} \text{ and } \mathcal{W}_l = w_l \text{ on } \partial G^{N,M}, \tag{20b}$$

$$\mathcal{L}^{N,M}\mathcal{W}_r = 0 \text{ on } G^{N,M} \text{ and } \mathcal{W}_r = w_r \text{ on } \partial G^{N,M}. \tag{20c}$$

5 Error analysis

In this section, we analyze the error between the continuous solution (6) and the discrete solution (18).

Lemma 5.1 *If v and $\mathcal{V}$ are the solutions of* (9a) *and* (20a) *respectively, then the smooth component satisfies the following error estimate,*

$$|(\mathcal{V} - v)(x_n, t_m)| \le C(N^{-1} + M^{-1}),\ \forall (x_n, t_m) \in \overline{G}^{\mathcal{N},\mathcal{M}}.$$

Proof From the usual truncation error argument and the bounds on the smooth component v and its derivatives given in the Theorem 3.4, we have:

$$|\mathcal{L}^{N,M}(\mathcal{V} - v)(x_n, t_m)| \le C_1 N^{-1}\left(\varepsilon\left\|\frac{\partial^3 v}{\partial x^3}\right\| + \mu\left\|\frac{\partial^2 v}{\partial x^2}\right\|\right) + C_2 M^{-1}\left\|\frac{\partial^2 v}{\partial t^2}\right\| \le C(N^{-1} + M^{-1}). \tag{21}$$

By using Lemma 4.2, we get the desired result. □

We shall now introduce the following two functions to establish the parameter-uniform error estimate for both the singular components:

$$\Psi_n^L = \begin{cases} \prod_{i=1}^{n}(1 + \rho_1 h_i)^{-1}, & 1 \le n \le N, \\ 1, & n = 0, \end{cases} \tag{22a}$$

$$\text{and } \Psi_n^R = \begin{cases} \prod_{i=n+1}^{N}(1 + \rho_2 h_i)^{-1}, & 1 \le n \le N, \\ 1, & n = N. \end{cases} \tag{22b}$$

Lemma 5.2 *If $\mathcal{W}_l$ and $\mathcal{W}_r$ are the solutions of* (20b) *and* (20c) *respectively, then we have the following bounds:*

$$|\mathcal{W}_l(x_n, t_m)| \le C\Psi_n^L, \quad \textit{and} \ |\mathcal{W}_r(x_n, t_m)| \le C\Psi_n^R. \tag{23}$$

Proof Consider the function $\xi_L^{\pm}(x_n, t_m) = \Psi_n^L \pm \mathcal{W}_l(x_n, t_m)$. Let $\overline{h_n} = \frac{h_{n+1}+h_n}{2}$. Using the properties

$$\Psi_n^L > 0,\ D_x^-\Psi_n^L = -\rho_1\Psi_n^L < 0,\ \text{and } \delta_x^2\Psi_n^L = \rho_1^2\Psi_{n+1}^L\frac{h_{n+1}}{\overline{h_n}} > 0,$$

we obtain

$$\mathcal{L}^{N,M}\xi_L^{\pm}(x_n, t_m) = -\varepsilon\delta_x^2\Psi_n^L + \mu b D_x^-\Psi_n^L + c\Psi_n^L = -\varepsilon\rho_1^2\Psi_{n+1}^L\frac{h_{n+1}}{\overline{h_n}} - \mu b\rho_1\Psi_n^L + c\Psi_n^L.$$

A simple calculation gives us

$$\mathcal{L}^{N,M}\xi_L^{\pm}(x_n, t_m) = \Psi_{n+1}^L\left(2\varepsilon\rho_1^2\left(1 - \frac{h_{n+1}}{2\overline{h_n}}\right) + (1 + \rho_1 h_{n+1})(-2\varepsilon\rho_1^2 - \mu b\rho_1 + c) + 2\varepsilon\rho_1^3 h_{n+1}\right).$$

Using the values of ρ_1 in the above expression, we can easily show that $\mathcal{L}^{N,M}\xi_L^{\pm}(x_n, t_m) \ge 0$ in both the cases and by applying Lemma 4.1, we obtain the required result.

Now, consider $\mathcal{L}^{N,M}\xi_R^{\pm}(x_n,t_m)=\Psi_n^R \pm \mathcal{W}_r(x_n,t_m)$. By using

$$\Psi_n^R>0,\ D_x^-\Psi_n^R=\frac{\rho_2}{1+\rho_2 h_n}\Psi_n^R>0 \text{ and } \delta_x^2\Psi_n^R=\frac{2\rho_2^2\Psi_n^R}{1+\rho_2 h_n}\left(1-\frac{h_{n+1}}{h_n+h_{n+1}}\right)>0,$$

we obtain

$$\mathcal{L}^{N,M}\xi_R^{\pm}(x_n,t_m)=\frac{\Psi_n^R}{1+\rho_2 h_n}\left(2\varepsilon\rho_2^2\frac{h_{n+1}}{h_n+h_{n+1}}+(-2\varepsilon\rho_2^2+\mu b\rho_2+c)+c\rho_2 h_n\right).$$

Again, we can easily see that $\mathcal{L}^{N,M}\xi_R^{\pm}(x_n,t_m)\geq 0$ for both the values of ρ_2 . Now, we apply Lemma 4.1 and obtain the desired bound. □

Lemma 5.3 *If w_l and $\mathcal{W}_l$ are the solutions of* (9b) *and* (20b) *respectively, then the left singular component satisfies the following error estimate,*

$$|(\mathcal{W}_l-w_l)(x_n,t_m)|\leq C_1N^{-1}ln\ N+C_2M^{-1},\ \forall(x_n,t_m)\in\overline{G}^{\mathcal{N},\mathcal{M}}.$$

Proof We shall use the classical argument to determine the local truncation error in the left singular component,

$$|\mathcal{L}^{N,M}(\mathcal{W}_l-w_l)(x_n,t_m)|\leq C_1(h_n+h_{n+1})\left(\varepsilon\left\|\frac{\partial^3 w_l}{\partial x^3}\right\|+\mu\left\|\frac{\partial^2 w_l}{\partial x^2}\right\|\right)+C_2M^{-1}\left\|\frac{\partial^2 w_l}{\partial t^2}\right\|. \tag{24}$$

The argument naturally splits in two cases:

Case 1: $\sigma_1=\frac{1}{4}$. The mesh is uniform in this case.
If $\mu^2\leq\frac{\zeta\varepsilon}{\beta}$, we have $\sqrt{\frac{\zeta\beta}{\varepsilon}}\leq 8\ lnN$ and then from Eq. (24), we get:

$$|\mathcal{L}^{N,M}(\mathcal{W}_l-w_l)(x_n,t_m)|\leq C_1N^{-1}ln\ N+C_2M^{-1}.$$

If $\mu^2\geq\frac{\zeta\varepsilon}{\beta}$, we have $\frac{\zeta}{\mu}\leq 8\ lnN$ and then from Eq. (24), we get:

$$|\mathcal{L}^{N,M}(\mathcal{W}_l-w_l)(x_n,t_m)|\leq C_1N^{-1}ln\ N+C_2M^{-1}.$$

Finally, the desired results for both the cases can be easily obtained by using Lemma 4.2.

Case 2: $\sigma_1<\frac{1}{4}$. The mesh is piece-wise uniform in this case.
Firstly, the coarse mesh region $(\sigma_1,1)\times(0,T)$ is considered. From Lemma 3.5 and by applying the inequality $ln(1+s)>s(1-s/2)$ with $s=4N^{-1}ln\ N$, we obtain:

$$|\mathcal{W}_l(x_{N/4},t_m)|\leq\Psi_{N/4}^L=\left(1+\rho_1\frac{4\sigma_1}{N}\right)^{-N/4}=\left(1+4\frac{ln\ N}{N}\right)^{-N/4}\leq CN^{-1}.$$

From Lemma 3.5, we have for both the choices of ρ_1, $|w_l(x,t)|\leq Ce^{-\rho_1 x}\leq Ce^{-\rho_1\sigma_1}\leq CN^{-1}$.
From these two results, we get:

$$|(\mathcal{W}_l-w_l)(x_n,t_m)|\leq CN^{-1}.$$

Now, consider the fine mesh region $(0,\sigma_1)\times(0,T)$. If $\mu^2\leq\frac{\zeta\varepsilon}{\beta}$, then we can get $h_n=h_{n+1}=\frac{8\sqrt{\varepsilon}}{\sqrt{\zeta\beta}}N^{-1}ln\ N$ by using the fact that $\sigma_1<\frac{1}{4}$. Then, Equation (24) reduces to

$$|\mathcal{L}^{N,M}(\mathcal{W}_l-w_l)(x_n,t_m)|\leq C(N^{-1}ln\ N+M^{-1}).$$

Next, if $\mu^2\geq\frac{\zeta\varepsilon}{\beta}$, then we have, $h_n=h_{n+1}=\frac{8\mu}{\zeta}N^{-1}ln\ N$. Then, Equation (24) reduces to

$$|\mathcal{L}^{N,M}(\mathcal{W}_l-w_l)(x_n,t_m)|\leq C(N^{-1}ln\ N+M^{-1}).$$

Use Lemma 4.2 to finish in both the cases.

□

Lemma 5.4 *If w_r and $\mathcal{W}_r$ are the solutions of* (9c) *and* (20c) *respectively, then the right singular component satisfies the following error estimate* $\forall (x_n, t_m) \in \overline{G}^{\mathcal{N},\mathcal{M}}$*:*

$$|(\mathcal{W}_r - w_r)(x_n, t_m)| \leq \begin{cases} C_1 N^{-1} ln\ N + C_2 M^{-1}, & \mu^2 \leq \frac{\zeta\varepsilon}{\beta}, \\ C_1 N^{-1} (ln\ N)^2 + C_2 M^{-1}, & \mu^2 \geq \frac{\zeta\varepsilon}{\beta}, \end{cases}$$

Proof

Case 1: $\sigma_2 = \frac{1}{4}$.
The mesh is uniform in this case.
If $\mu^2 \leq \frac{\zeta\varepsilon}{\beta}$, we have $\sqrt{\frac{\zeta\beta}{\varepsilon}} \leq 8\ ln\ N$ and then from Eq. (24), we get:

$$|\mathcal{L}^{N,M}(\mathcal{W}_r - w_r)(x_n, t_m)| \leq C_1 N^{-1} ln\ N + C_2 M^{-1}.$$

If $\mu^2 \geq \frac{\zeta\varepsilon}{\beta}$, we have $\frac{\mu\beta}{\varepsilon} \leq 8\ ln\ N$ and then from Equation (24), we get:

$$|\mathcal{L}^{N,M}(\mathcal{W}_r - w_r)(x_n, t_m)| \leq C_1 N^{-1} (ln\ N)^2 + C_2 M^{-1}.$$

Use Lemma 4.2 to finish in both the cases.

Case 2: $\sigma_2 < \frac{1}{4}$.
The mesh is piece-wise uniform in this case.
Firstly, we consider the coarse mesh region $(0, 1-\sigma_2] \times (0, T)$. From Lemma 3.5, we have

$$|\mathcal{W}_r(x_{3N/4}, t_m)| \leq \Psi^R_{3N/4} = \left(1 + \rho_2 \frac{4\sigma_2}{N}\right)^{-N/4} = \left(1 + 4\frac{ln\ N}{N}\right)^{-N/4} \leq CN^{-1},$$

by using the same arguments as w_l.
From Lemma 3.5, we have for both the choices of ρ_2,

$$|w_r(x, t)| \leq Ce^{-\rho_2(1-x)} \leq Ce^{-\rho_2\sigma_2} \leq CN^{-1}.$$

From these two results, we obtain

$$|(\mathcal{W}_r - w_r)(x_n, t_m)| \leq CN^{-1}.$$

Now, the fine mesh region $(1-\sigma_2, 1) \times (0, T)$ is considered. We start with the case $\mu^2 \leq \frac{\zeta\varepsilon}{\beta}$. As in the case of $\mathcal{W}_l$, we can get $h_n = h_{n+1} = \frac{8\sqrt{\varepsilon}}{\sqrt{\zeta\beta}} N^{-1} ln\ N$. Then, Eq. (24) reduces to

$$|\mathcal{L}^{N,M}(\mathcal{W}_r - w_r)(x_n, t_m)| \leq C_1 N^{-1} ln\ N + C_2 M^{-1}.$$

Next, we consider the case of $\mu^2 \geq \frac{\zeta\varepsilon}{\beta}$. Here, $h_n = h_{n+1} = \frac{8\varepsilon}{\mu\beta} N^{-1} ln\ N$. Then, Eq. (24) reduces to

$$|\mathcal{L}^{N,M}(\mathcal{W}_r - w_r)(x_n, t_m)| \leq C_1 N^{-1} \frac{\mu^2}{\varepsilon} ln\ N + C_2 M^{-1}.$$

Now, we can construct the following barrier function, for sufficiently large C,

$$\xi^{\pm}(x_n, t_m) = C\left(N^{-1} ln\ N + N^{-1} ln\ N\left((x_n - (1-\sigma_2))\frac{\mu}{\varepsilon}\right) + M^{-1}\right) \pm (\mathcal{W}_r - w_r)(x_n, t_m).$$

We can clearly see that both the functions $\xi^{\pm}(x_n, t_m)$ are non-negative at all points of $G^{N,M}$ of the form $(1, t_m)$, $(x_{3N/4}, t_m)$ and $(x_n, 0)$. Also, we have $\mathcal{L}^{N,M}\xi^{\pm} \geq 0$. Therefore, by applying Lemma 4.1, we obtain:

$$|(\mathcal{W}_r - w_r)(x_n, t_m)| \leq C\left(N^{-1} ln\ N + N^{-1} ln\ N\left((x_n - (1-\sigma_2))\frac{\mu}{\varepsilon}\right) + M^{-1}\right).$$

Finally, using $\sigma_2 = \frac{2\varepsilon}{\mu\beta} ln\ N$, we get:

$$|(\mathcal{W}_r - w_r)(x_n, t_m)| \leq C_1 N^{-1} (ln\ N)^2 + C_2 M^{-1}.$$

□

Theorem 5.5 *If y and $\mathcal{Y}$ are the solutions of* (5) *and* (18) *respectively, then* $\forall (x_n, t_m) \in \overline{G}^{\mathcal{N},\mathcal{M}}$,

$$||\mathcal{Y} - y|| \leq \begin{cases} C_1 N^{-1} ln\ N + C_2 M^{-1}, & \mu^2 \leq \frac{\zeta\varepsilon}{\beta}, \\ C_1 N^{-1} (ln\ N)^2 + C_2 M^{-1}, & \mu^2 \geq \frac{\zeta\varepsilon}{\beta}. \end{cases}$$

Proof The proof follows from Lemma 5.1, 5.3 and 5.4 where the error in the discrete solution can be decomposed as:

$$(\mathcal{Y} - y)(x_n, t_m) = ((\mathcal{V} - v) + (\mathcal{W}_l - w_l) + (\mathcal{W}_r - w_r))(x_n, t_m).$$

□

6 Numerical results

We analyze two test examples, in this section, to corroborate in practice the accuracy of the numerical scheme (18) and the theoretical analysis. Since the exact solutions of these test examples are unknown, the two-mesh method [3] is used to compute the global orders of convergence.

The maximum point-wise two-mesh difference is defined as follows:

$$D^N_{\varepsilon,\mu} = ||\mathcal{Y}^N_{\varepsilon,\mu} - \overline{\mathcal{Y}}^{2N}_{\varepsilon,\mu}||_{G^{N,M}},$$

where $\overline{\mathcal{Y}}^N_{\varepsilon,\mu}$ are the piece-wise linear interpolants of the numerical solutions $\mathcal{Y}^N_{\varepsilon,\mu}$.

The ε-uniform maximum point-wise two mesh differences D^N_μ and the (ε, μ)-uniform maximum point-wise two-mesh differences D^N are computed as follows:

$$D^N_\mu = \max_{\varepsilon \in R_\varepsilon} D^N_{\varepsilon,\mu}, \ D^N = \max_{\mu \in R_\mu} \max_{\varepsilon \in R_\varepsilon} D^N_{\varepsilon,\mu},$$

where $R_\varepsilon = \{2^{-1}, \ldots, 2^{-26}\}$ and $R_\mu = \{2^{-1}, 2^{-2}, \ldots, 2^{-26}\}$.

The order of local convergence $p^N_{\varepsilon,\mu}$, the ε-uniform order of local convergence p^N_μ and the (ε, μ)-uniform order of convergence p^N are computed as follows:

$$p^N_{\varepsilon,\mu} = \log_2\left(\frac{D^N_{\varepsilon,\mu}}{D^{2N}_{\varepsilon,\mu}}\right), \ p^N_\mu = \log_2\left(\frac{D^N_\mu}{D^{2N}_\mu}\right), \text{ and } p^N = \log_2\left(\frac{D^N}{D^{2N}}\right).$$

Example 6.1 Consider the problem,

$$\begin{cases} \frac{\partial u}{\partial t} - \varepsilon \frac{\partial^2 u}{\partial x^2} + \mu(1 + t^2)\frac{\partial u}{\partial x} + u = 16x^2(1 - x)^2, \ (x, t) \in G = (0, 1) \times (0, 1], \\ u(x, 0) = \begin{cases} -x^3, & \text{if } \ 0 \leq x < 0.3, \\ (1 - x)^3, & \text{if } \ 0.3 \leq x \leq 1, \end{cases} \\ u(0, t) = 0 = u(1, t), \ 0 < t \leq 1. \end{cases} \tag{25}$$

The characteristic curve Ω is given by $p(t) = \mu(t + t^3/3) + 0.3$. The numerical results for y and u with different values of parameters ε and μ are presented in Figs. 1 and 2. In both figures, the interior layer is distinctly observed at $x = 0.3$ which emerges due to the discontinuous initial condition. The log–log plots provided in Fig. 3 demonstrate clear evidence of first-order convergence. Furthermore, the numerical data shown in Tables 1 through 6 agrees well with the theoretical asymptotic error bound suggested in Theorem 5.5.

Specifically, Tables 1, 3, and 5 illustrate first-order convergence in the time variable, achieved by setting $M = N$ and Tables 2, 4, and 6 show first-order convergence in the spatial variable, obtained by setting $M = 4N$.

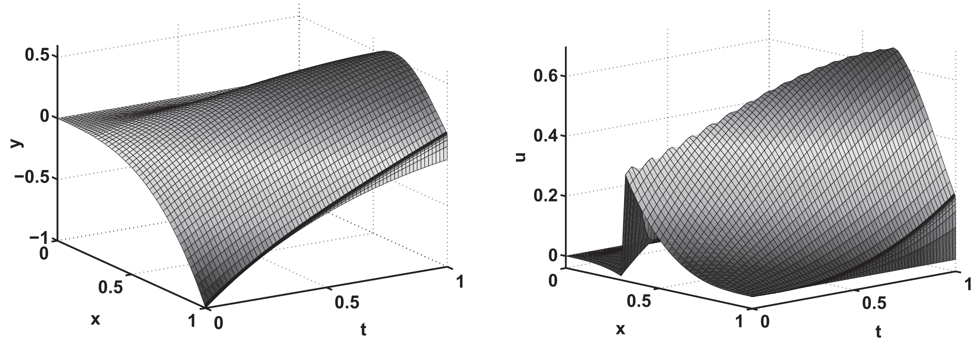

(a) (b)

Fig. 1 Numerical solution to **a** y and **b** u for Example 6.1 when $\varepsilon = 2^{-12}$, $\mu = 2^{-2}$ and $N = M = 64$

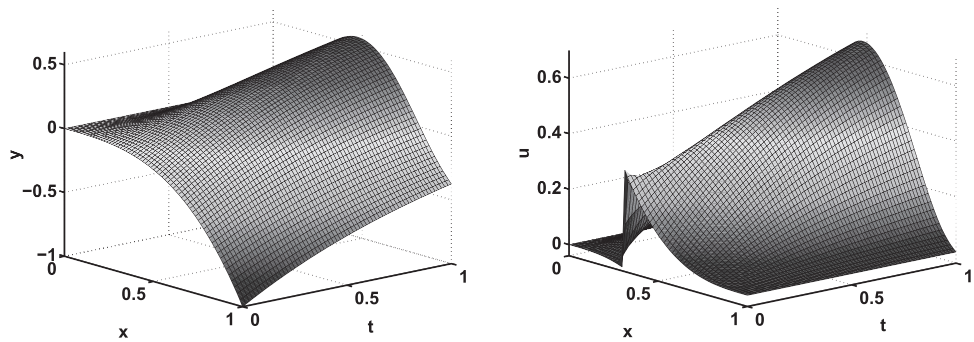

(a) (b)

Fig. 2 Numerical solution to **a** y and **b** u for Example 6.1 when $\varepsilon = 2^{-8}$, $\mu = 2^{-12}$ and $N = M = 64$

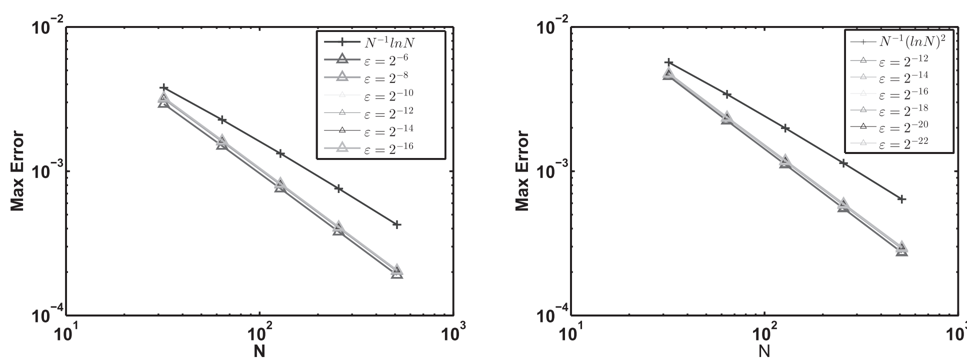

(a) $\mu = 2^{-26}$ (b) $\mu = 2^{-6}$

Fig. 3 Log–log plots for maximum errors vs $N = \{32, 64, 128, 256, 512\}$ for Example 6.1

Example 6.2 Consider the problem,

$$\begin{cases} \frac{\partial u}{\partial t} - \varepsilon \frac{\partial^2 u}{\partial x^2} + \mu(1 + e^t)\frac{\partial u}{\partial x} + (1 + t)u = x(1 - x)(e^t - 1), \ (x, t) \in G = (0, 1) \times (0, 1], \\ u(x, 0) = \begin{cases} -x^5, & \text{if} \ \ 0 \le x < 0.1, \\ (1 - x)^5, & \text{if} \ \ 0.1 \le x \le 1, \end{cases} \\ u(0, t) = 0 = u(1, t), \ 0 < t \le 1. \end{cases} \tag{26}$$

The characteristic curve Ω is given by $p(t) = \mu(t + e^t - 1) + 0.1$. The numerical results for y and u with different values of parameters ε and μ are presented in Figs. 4 and 5. The numerical results presented in Tables 7,

Table 1 $D^N_{\varepsilon,\mu}$ and $p^N_{\varepsilon,\mu}$ for the solution y of Example 6.1 using scheme (18) for $\mu = 2^{-4}$ when $M = N$

	$N = M = 8$	$N = M = 16$	$N = M = 32$	$N = M = 64$	$N = M = 128$	$N = M = 256$	$N = M = 512$
$\varepsilon = 2^{-2}$	8.3836e−03	4.7759e−03	2.1888e−03	1.1046e−03	7.8397e−04	5.4630e−04	3.8124e−04
	0.8118	1.1256	0.9866	0.4947	0.5211	0.5190	
$\varepsilon = 2^{-4}$	1.4090e−02	7.7583e−03	4.0868e−03	2.0938e−03	1.0591e−03	5.3254e−04	2.6700e−04
	0.8608	0.9248	0.9649	0.9833	0.9918	0.9960	
$\varepsilon = 2^{-6}$	2.2343e−02	1.1909e−02	6.1925e−03	3.1540e−03	1.5906e−03	7.9861e−04	4.0013e−04
	0.9078	0.9435	0.9733	0.9876	0.9940	0.9970	
$\varepsilon = 2^{-8}$	2.6078e−02	1.3719e−02	7.0384e−03	3.5573e−03	1.7873e−03	8.9593e−04	4.4851e−04
	0.9266	0.9628	0.9845	0.9930	0.9964	0.9982	
$\varepsilon = 2^{-10}$	3.1299e−02	1.6455e−02	8.2745e−03	4.0984e−03	2.0181e−03	9.9078e−04	4.8566e−04
	0.9276	0.9918	1.0136	1.0221	1.0264	1.0286	
$\varepsilon = 2^{-12}$	3.3101e−02	1.7471e−02	8.9236e−03	4.4918e−03	2.2464e−03	1.1206e−03	5.5831e−04
	0.9219	0.9693	0.9903	0.9997	1.0034	1.0051	
$\varepsilon = 2^{-14}$	3.3532e−02	1.7692e−02	9.0969e−03	4.5890e−03	2.3040e−03	1.1533e−03	5.7665e−04
	0.9224	0.9597	0.9872	0.9940	0.9984	0.9999	
$\vdots$	$\vdots$	$\vdots$	$\vdots$	$\vdots$	$\vdots$	$\vdots$	$\vdots$
$\varepsilon = 2^{-26}$	3.3674e−02	1.7763e−02	9.1526e−03	4.6197e−03	2.3229e−03	1.1643e−03	5.8278e−04
	0.9228	0.9566	0.9864	0.9919	0.9965	0.9984	
$D^N_{\mu=2^{-4}}$	3.3674e−02	1.7763e−02	9.1526e−03	4.6197e−03	2.3229e−03	1.1643e−03	5.8278e−04
$p^N_{\mu=2^{-4}}$	0.9228	0.9566	0.9864	0.9919	0.9965	0.9984	

Table 2 $D^N_{\varepsilon,\mu}$ and $p^N_{\varepsilon,\mu}$ for the solution y of Example 6.1 using scheme (18) for $\mu = 2^{-4}$ when $M = 4N$

	$N = 8$ $M = 32$	$N = 16$ $M = 64$	$N = 32$ $M = 128$	$N = 64$ $M = 256$	$N = 128$ $M = 512$	$N = 256$ $M = 1024$	$N = 512$ $M = 2048$
$\varepsilon = 2^{-2}$	2.7442e−03	1.5145e−03	9.3625e−04	5.9863e−04	4.0063e−04	2.7339e−04	1.9127e−04
	0.8575	0.6939	0.6452	0.5794	0.5513	0.5153	
$\varepsilon = 2^{-4}$	8.3340e−03	4.6997e−03	2.4860e−03	1.2785e−03	6.4844e−04	3.2651e−04	1.6383e−04
	0.8264	0.9187	0.9594	0.9794	0.9899	0.9949	
$\varepsilon = 2^{-6}$	1.3819e−02	7.3693e−03	3.8347e−03	1.9532e−03	9.8527e−04	4.9488e−04	2.4800e−04
	0.9071	0.9424	0.9733	0.9872	0.9934	0.9968	
$\varepsilon = 2^{-8}$	1.6784e−02	8.6961e−03	4.4619e−03	2.2541e−03	1.1321e−03	5.6726e−04	2.8394e−04
	0.9486	0.9627	0.9851	0.9935	0.9969	0.9984	
$\varepsilon = 2^{-10}$	2.1670e−02	1.1343e−02	5.6539e−03	2.7779e−03	1.3538e−03	6.5775e−04	3.1890e−04
	0.9339	1.0045	1.0252	1.0370	1.0414	1.0444	
$\varepsilon = 2^{-12}$	2.3562e−02	1.2450e−02	6.2893e−03	3.1664e−03	1.5808e−03	7.8687e−04	3.9124e−04
	0.9203	0.9852	0.9900	1.0022	1.0064	1.0081	
$\varepsilon = 2^{-14}$	2.4024e−02	1.2702e−02	6.4683e−03	3.2662e−03	1.6380e−03	8.1942e−04	4.0952e−04
	0.9195	0.9736	0.9858	0.9956	0.9993	1.0007	
$\vdots$	$\vdots$	$\vdots$	$\vdots$	$\vdots$	$\vdots$	$\vdots$	$\vdots$
$\varepsilon = 2^{-26}$	2.4177e−02	1.2783e−02	6.5277e−03	3.2997e−03	1.6569e−03	8.3035e−04	4.1562e−04
	0.9194	0.9696	0.9843	0.9939	0.9967	0.9984	
$D^N_{\mu=2^{-4}}$	2.4177e−02	1.2783e−02	6.5277e−03	3.2997e−03	1.6569e−03	8.3035e−04	4.1562e−04
$p^N_{\mu=2^{-4}}$	0.9194	0.9696	0.9843	0.9939	0.9967	0.9984	

8 and 9 and log–log plots presented in Fig. 6 correspond with the asymptotic error bound that is theoretically proposed in the Theorem 5.5.

Log–log plots for maximum errors vs $N = \{32, 64, 128, 256, 512\}$ for Example 6.2

7 Conclusions

In this study, we thoroughly investigated and analyzed a class of TP-SPPs of the form (1), where the convective coefficient $b(\equiv b(t))$ is a function solely of the time variable t, and the initial function $\chi(x)$ exhibits a jump discontinuity at the point $(p, 0)$. This discontinuity induces the presence of an interior layer. To address this, we

Table 3 $D^N_{\varepsilon,\mu}$ and $p^N_{\varepsilon,\mu}$ for the solution y of Example 6.1 using scheme (18) for $\mu = 2^{-12}$ when $M = N$

	$N=M=8$	$N=M=16$	$N=M=32$	$N=M=64$	$N=M=128$	$N=M=256$	$N=M=512$
$\varepsilon = 2^{-2}$	8.5768e−03 0.7853	4.9766e−03 1.1683	2.2143e−03 0.9920	1.1133e−03 0.4609	8.0885e−04 0.5165	5.6545e−04 0.5106	3.9692e−04
$\varepsilon = 2^{-4}$	6.8825e−03 0.7710	4.0332e−03 0.8958	2.1677e−03 0.9504	1.1217e−03 0.9759	5.7030e−04 0.9886	2.8741e−04 0.9946	1.4424e−04
$\varepsilon = 2^{-6}$	1.0007e−02 0.8384	5.5969e−03 0.9323	2.9328e−03 0.9653	1.5021e−03 0.9833	7.5979e−04 0.9917	3.8209e−04 0.9958	1.9160e−04
$\varepsilon = 2^{-8}$	1.1284e−02 0.8683	6.1812e−03 0.9594	3.1788e−03 0.9804	1.6111e−03 0.9900	8.1113e−04 0.9951	4.0694e−04 0.9975	2.0382e−04
$\varepsilon = 2^{-10}$	1.1784e−02 0.9092	6.2746e−03 0.9587	3.2285e−03 0.9822	1.6343e−03 0.9927	8.2130e−04 0.9967	4.1159e−04 0.9982	2.0606e−04
$\varepsilon = 2^{-12}$	1.1997e−02 0.9306	6.2940e−03 0.9528	3.2517e−03 0.9859	1.6419e−03 0.9926	8.2514e−04 0.9967	4.1352e−04 0.9986	2.0697e−04
$\varepsilon = 2^{-14}$	1.2064e−02 0.9397	6.2896e−03 0.9483	3.2596e−03 0.9863	1.6454e−03 0.9932	8.2656e−04 0.9967	4.1423e−04 0.9984	2.0735e−04
$\vdots$	$\vdots$	$\vdots$	$\vdots$	$\vdots$	$\vdots$	$\vdots$	$\vdots$
$\varepsilon = 2^{-26}$	1.2098e−02 0.9445	6.2860e−03 0.9458	3.2634e−03 0.9864	1.6472e−03 0.9932	8.2747e−04 0.9964	4.1477e−04 0.9983	2.0763e−04
$D^N_{\mu=2^{-12}}$	1.2098e−02	6.2860e−03	3.2634e−03	1.6472e−03	8.2747e−04	4.1477e−04	2.0763e−04
$p^N_{\mu=2^{-12}}$	0.9445	0.9458	0.9864	0.9932	0.9964	0.9983	

Table 4 $D^N_{\varepsilon,\mu}$ and $p^N_{\varepsilon,\mu}$ for the solution y of Example 6.1 using scheme (18) for $\mu = 2^{-12}$ when $M = 4N$

	$N=8$ $M=32$	$N=16$ $M=64$	$N=32$ $M=128$	$N=64$ $M=256$	$N=128$ $M=512$	$N=256$ $M=1024$	$N=512$ $M=2048$
$\varepsilon = 2^{-2}$	2.6785e−03 0.8009	1.5375e−03 0.6792	9.6015e−04 0.6331	6.1910e−04 0.5712	4.1670e−04 0.5472	2.8517e−04 0.5109	2.0013e−04
$\varepsilon = 2^{-4}$	2.3524e−03 1.3226	9.4052e−04 0.9478	4.8758e−04 0.8695	2.6687e−04 0.7447	1.5926e−04 0.6313	1.0282e−04 0.5681	6.9352e−05
$\varepsilon = 2^{-6}$	3.6042e−03 1.3022	1.4616e−03 1.0557	7.0312e−04 0.9295	3.6918e−04 0.9644	1.8920e−04 0.9820	9.5789e−05 0.9910	4.8196e−05
$\varepsilon = 2^{-8}$	3.5531e−03 1.2020	1.5445e−03 0.9495	7.9974e−04 0.9760	4.0658e−04 0.9877	2.0503e−04 0.9940	1.0295e−04 0.9970	5.1581e−05
$\varepsilon = 2^{-10}$	3.2624e−03 1.0216	1.6070e−03 0.9603	8.2587e−04 0.9864	4.1684e−04 0.9967	2.0890e−04 1.0002	1.0443e−04 0.9994	5.2240e−05
$\varepsilon = 2^{-12}$	3.1798e−03 0.9513	1.6444e−03 0.9679	8.4075e−04 0.9946	4.2197e−04 0.9980	2.1128e−04 0.9999	1.0565e−04 1.0008	5.2797e−05
$\varepsilon = 2^{-14}$	3.2419e−03 0.9693	1.6558e−03 0.9675	8.4678e−04 0.9965	4.2441e−04 0.9988	2.1239e−04 0.9998	1.0621e−04 1.0002	5.3096e−05
$\vdots$	$\vdots$	$\vdots$	$\vdots$	$\vdots$	$\vdots$	$\vdots$	$\vdots$
$\varepsilon = 2^{-26}$	3.2689e−03 0.9782	1.6593e−03 0.9644	8.5035e−04 0.9970	4.2605e−04 0.9986	2.1323e−04 0.9989	1.0669e−04 0.9997	5.3357e−05
$D^N_{\mu=2^{-12}}$	3.2689e−03	1.6593e−03	8.5035e−04	4.2605e−04	2.1323e−04	1.0669e−04	5.3357e−05
$p^N_{\mu=2^{-12}}$	0.9782	0.9644	0.9970	0.9986	0.9989	0.9997	

introduced a singular function $\mathcal{A}(x, t)$ and subtracted it from the solution u of the original problem (1), resulting in a new function y with a continuous initial condition.

The numerical method comprising of standard central differences and the backward Euler method is applied on the mesh $\overline{G}^{N,M}$ which employs a uniform mesh for the time variable and a piece-wise uniform mesh for the space variable, with clearly defined transition points. Error analysis revealed that our proposed numerical scheme achieves first-order convergence in both time and space variables, independent of the perturbation parameters. To substantiate our theoretical claims, we conducted numerical experiments on two test problems with unknown exact solutions. Detailed results from these experiments are presented in Tables 1 through 9, confirming the parameter-uniform convergence of our scheme. Additionally, corresponding graphs are provided in Figs. 1 through 6 to visually support our findings.

Table 5 The ε-uniform orders of local convergence p_{μ}^{N} and the $(\varepsilon, \mu)-$uniform orders of local convergence p^{N} for the solution y using scheme (18) when $N = M$

	$N = M = 8$	$N = M = 16$	$N = M = 32$	$N = M = 64$	$N = M = 128$	$N = M = 256$
$\mu = 2^{-2}$	0.7769	0.8296	0.7779	0.5389	0.6828	0.7289
$\mu = 2^{-4}$	0.9228	0.9566	0.9864	0.9919	0.9965	0.9984
$\mu = 2^{-6}$	0.9613	1.0005	1.0112	0.9950	0.9981	0.9990
$\mu = 2^{-10}$	0.9396	0.9503	0.9876	0.9925	0.9969	0.9986
$\mu = 2^{-12}$	0.9445	0.9458	0.9864	0.9932	0.9964	0.9983
$\mu = 2^{-14}$	0.9460	0.9446	0.9862	0.9930	0.9965	0.9982
$\mu = 2^{-18}$	0.9463	0.9446	0.9861	0.9930	0.9965	0.9982
$\mu = 2^{-22}$	0.9463	0.9446	0.9861	0.9930	0.9965	0.9982
$\mu = 2^{-26}$	0.9463	0.9446	0.9861	0.9930	0.9965	0.9982
p^{N}	0.9463	0.9446	0.9861	0.9930	0.9965	0.9982

Table 6 The ε-uniform orders of local convergence p_{μ}^{N} and the $(\varepsilon, \mu)-$uniform orders of local convergence p^{N} for the solution y using scheme (18) when $M = 4N$

	$N = 8$ $M = 32$	$N = 16$ $M = 64$	$N = 32$ $M = 128$	$N = 64$ $M = 256$	$N = 128$ $M = 512$	$N = 256$ $M = 1024$
$\mu = 2^{-2}$	0.8036	0.8343	0.5978	0.5152	0.6714	0.7259
$\mu = 2^{-4}$	0.9194	0.9696	0.9843	0.9939	0.9967	0.9984
$\mu = 2^{-6}$	0.9692	1.0389	1.0382	0.9978	0.9995	0.9998
$\mu = 2^{-10}$	0.9584	0.9651	0.9989	0.9979	1.0001	1.0003
$\mu = 2^{-12}$	0.9782	0.9644	0.9970	0.9986	0.9989	0.9997
$\mu = 2^{-14}$	0.9841	0.9646	0.9966	0.9983	0.9992	0.9995
$\mu = 2^{-18}$	0.9860	0.9651	0.9965	0.9982	0.9991	0.9995
$\mu = 2^{-22}$	0.9861	0.9651	0.9965	0.9982	0.9991	0.9995
$\mu = 2^{-26}$	0.9861	0.9651	0.9965	0.9982	0.9991	0.9995
p^{N}	0.9861	0.9651	0.9965	0.9982	0.9991	0.9995

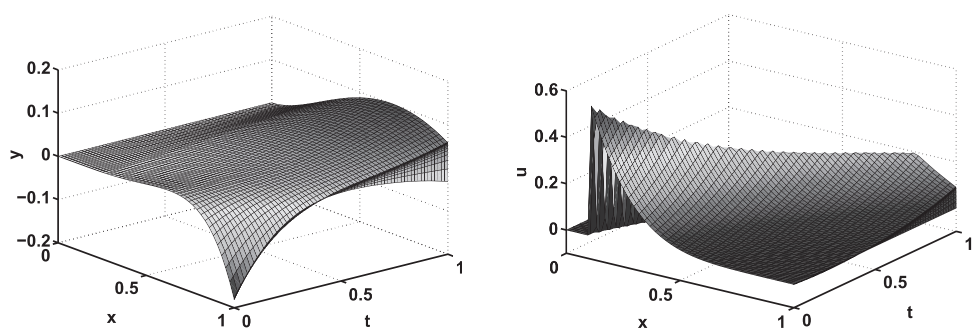

(a) (b)

Fig. 4 Numerical solution to **a** y and **b** u for Example 6.2 when $\varepsilon = 2^{-12},\ \mu = 2^{-2}$ and $N = M = 64$

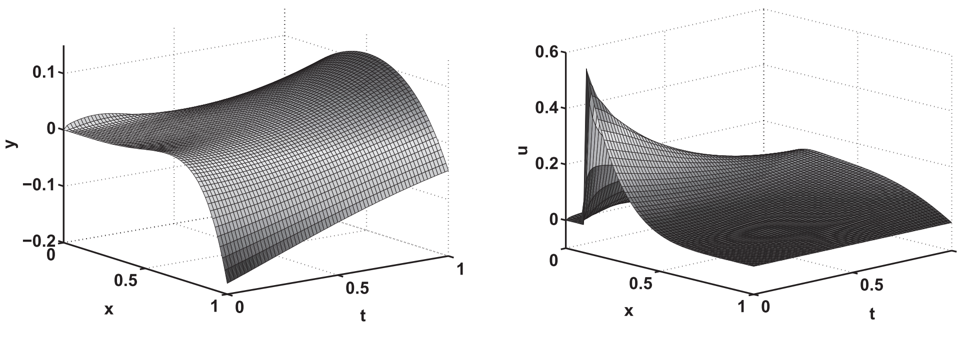

Fig. 5 Numerical solution to **a** y and **b** u for Example 6.2 when $\varepsilon = 2^{-8}$, $\mu = 2^{-12}$ and $N = M = 64$

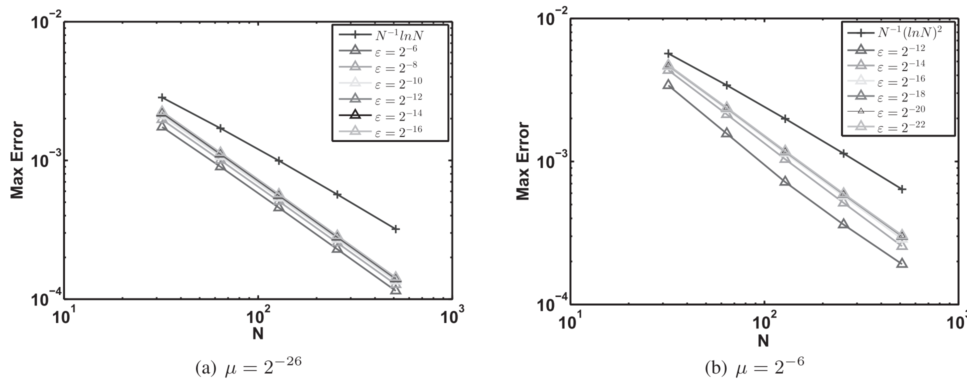

Fig. 6 Log-log plots for maximum errors vs $N = \{32, 64, 128, 256, 512\}$ for example 6.2

Table 7 $D^N_{\varepsilon,\mu}$ and $p^N_{\varepsilon,\mu}$ for the solution y of Example 6.2 using scheme (18) for $\mu = 2^{-4}$

	$N = M = 8$	$N = M = 16$	$N = M = 32$	$N = M = 64$	$N = M = 128$	$N = M = 256$	$N = M = 512$
$\varepsilon = 2^{-2}$	5.3693e−03 0.8589	2.9604e−03 1.0036	1.4765e−03 0.4499	1.0809e−03 0.5718	7.2721e−04 0.5428	4.9918e−04 0.5243	3.4708e−04
$\varepsilon = 2^{-4}$	4.2330e−03 0.7091	2.5893e−03 0.8694	1.4173e−03 0.9462	7.3560e−04 0.9738	3.7453e−04 0.9871	1.8895e−04 0.9935	9.4901e−05
$\varepsilon = 2^{-6}$	7.2317e−03 0.6304	4.6716e−03 0.8191	2.6479e−03 0.9112	1.4079e−03 0.9558	7.2589e−04 0.9787	3.6834e−04 0.9897	1.8549e−04
$\varepsilon = 2^{-8}$	1.1098e−02 1.0830	5.2388e−03 0.7355	3.1464e−03 0.7328	1.8933e−03 0.9436	9.8439e−04 0.9698	5.0260e−04 0.9844	2.5404e−04
$\varepsilon = 2^{-10}$	1.8577e−02 0.8747	1.0131e−02 1.0253	4.9777e−03 1.0687	2.3732e−03 1.0212	1.1693e−03 1.0487	5.6524e−04 1.0613	2.7086e−04
$\varepsilon = 2^{-12}$	2.0732e−02 0.7895	1.1994e−02 0.9231	6.3255e−03 0.9880	3.1892e−03 0.9965	1.5985e−03 0.9837	8.0831e−04 1.0009	4.0391e−04
$\varepsilon = 2^{-14}$	2.1261e−02 0.7663	1.2500e−02 0.8888	6.7505e−03 0.9534	3.4859e−03 0.9800	1.7673e−03 0.9902	8.8969e−04 0.9940	4.4670e−04
⋮	⋮	⋮	⋮	⋮	⋮	⋮	⋮
$\varepsilon = 2^{-26}$	2.1436e−02 0.7586	1.2670e−02 0.8766	6.9011e−03 0.9401	3.5968e−03 0.9715	1.8343e−03 0.9862	9.2599e−04 0.9931	4.6520e−04
$p^N_{\mu=2^{-4}}$	0.7586	0.8766	0.9401	0.9715	0.9862	0.9931	

Table 8 $D^N_{\varepsilon,\mu}$ and $p^N_{\varepsilon,\mu}$ for the solution y of Example 6.2 using scheme (18) for $\mu = 2^{-12}$

	$N = M = 8$	$N = M = 16$	$N = M = 32$	$N = M = 64$	$N = M = 128$	$N = M = 256$	$N = M = 512$
$\varepsilon = 2^{-2}$	5.0794e−03	3.1824e−03	1.6007e−03	1.1052e−03	7.5378e−04	5.2166e−04	3.6455e−04
	0.6746	0.9914	0.5344	0.5521	0.5310	0.5170	
$\varepsilon = 2^{-4}$	2.3043e−03	1.3386e−03	6.5555e−04	3.8868e−04	2.4254e−04	1.6424e−04	1.1194e−04
	0.7836	1.0299	0.7541	0.6803	0.5624	0.5531	
$\varepsilon = 2^{-6}$	6.7901e−04	4.1172e−04	2.2641e−04	1.1841e−04	6.0535e−05	3.0603e−05	1.5385e−05
	0.7218	0.8627	0.9351	0.9679	0.9841	0.9921	
$\varepsilon = 2^{-8}$	6.6820e−04	3.5594e−04	1.8292e−04	9.2718e−05	4.6685e−05	2.3421e−05	1.1730e−05
	0.9086	0.9604	0.9803	0.9899	0.9952	0.9976	
$\varepsilon = 2^{-10}$	6.6020e−04	3.4484e−04	1.7747e−04	8.9605e−05	4.4987e−05	2.2533e−05	1.1276e−05
	0.9370	0.9584	0.9859	0.9941	0.9975	0.9988	
$\varepsilon = 2^{-12}$	7.2300e−04	3.7624e−04	1.9817e−04	1.0238e−04	5.2521e−05	2.6588e−05	1.3407e−05
	0.9424	0.9249	0.9527	0.9630	0.9821	0.9877	
$\varepsilon = 2^{-14}$	8.4887e−04	4.2759e−04	2.2255e−04	1.1316e−04	5.7196e−05	2.8764e−05	1.4454e−05
	0.9893	0.9421	0.9757	0.9844	0.9916	0.9928	
$\vdots$	$\vdots$	$\vdots$	$\vdots$	$\vdots$	$\vdots$	$\vdots$	$\vdots$
$\varepsilon = 2^{-26}$	1.1125e−03	5.6619e−04	2.8589e−04	1.4366e−04	7.2004e−05	3.6038e−05	1.8023e−05
	0.9745	0.9858	0.9928	0.9966	0.9986	0.9996	
$p^N_{\mu=2^{-12}}$	0.9745	0.9858	0.9928	0.9966	0.9986	0.9996	

Table 9 The ε-uniform orders of local convergence p^N_μ and the $(\varepsilon, \mu)-$uniform orders of local convergence p^N for the solution y using scheme (18)

	$N = M = 8$	$N = M = 16$	$N = M = 32$	$N = M = 64$	$N = M = 128$	$N = M = 256$
$\mu = 2^{-2}$	0.6971	0.8450	0.9331	0.9708	0.9860	0.9931
$\mu = 2^{-4}$	0.7586	0.8766	0.9401	0.9715	0.9862	0.9931
$\mu = 2^{-6}$	0.7988	0.9301	0.9953	1.0237	0.9875	0.9938
$\mu = 2^{-10}$	0.9072	0.9503	0.9749	0.9880	0.9947	0.9982
$\mu = 2^{-12}$	0.9745	0.9858	0.9928	0.9966	0.9986	0.9996
$\mu = 2^{-14}$	1.0005	1.0009	1.0013	1.0015	1.0016	1.0017
$\mu = 2^{-18}$	1.0092	1.0051	1.0018	1.0008	1.0004	1.0002
$\mu = 2^{-22}$	1.0087	1.0036	1.0018	1.0008	1.0004	1.0002
$\mu = 2^{-26}$	1.0086	1.0036	1.0018	1.0008	1.0004	1.0002
p^N	1.0087	1.0036	1.0018	1.0008	1.0004	1.0002

Future research will focus on extending these findings to cases where the convective coefficient b is a function of both time and space variables ($b \equiv b(x, t)$). This extension aims to enhance the applicability and robustness of our numerical methods in more complex and realistic models of singularly perturbed differential equations.

Declarations

Conflict of interest The author declare that he has no competing interests.

References

1. Bobisud, L. E. Parabolic equations with a small parameter and discontinuous data. *Journal of Mathematical Analysis and Applications 26*, 1 (1969), 208–220.
2. Das, P., and Mehrmann, V. Numerical solution of singularly perturbed convection-diffusion-reaction problems with two small parameters. *BIT Numerical Mathematics 56* (2016), 51–76.
3. Farrell, P., Hegarty, A., Miller, J. M., O'Riordan, E., and Shishkin, G. I. *Robust computational techniques for boundary layers*. CRC Press, 2000.
4. Gracia, J. L., and O'Riordan, E. Parameter-uniform approximations for a singularly perturbed convection-diffusion problem with a discontinuous initial condition. *Applied Numerical Mathematics 162* (2021), 106–123.
5. Gracia, J. L., O'Riordan, E., and Pickett, M. A parameter robust second order numerical method for a singularly perturbed two-parameter problem. *Applied Numerical Mathematics 56*, 7 (2006), 962–980.

6. Gracia, J. L., and O'Riordan, E. Singularly perturbed reaction–diffusion problems with discontinuities in the initial and/or the boundary data. *Journal of Computational and Applied Mathematics 370* (2020), 112638.
7. Gracia, J. L., and O'Riordan, E. Numerical approximations to a singularly perturbed convection-diffusion problem with a discontinuous initial condition. *Numerical Algorithms 88*, 4 (2021), 1851–1873.
8. Gupta, V., Kadalbajoo, M. K., and Dubey, R. K. A parameter-uniform higher order finite difference scheme for singularly perturbed time-dependent parabolic problem with two small parameters. *International Journal of Computer Mathematics 96*, 3 (2019), 474–499.
9. Hemker, P., and Shishkin, G. Discrete approximation of singularly perturbed parabolic pdes with a discontinuous initial condition. In *Bail VI Proceedings* (1994), pp. 3–4.
10. Jha, A., and Kadalbajoo, M. K. A robust layer adapted difference method for singularly perturbed two-parameter parabolic problems. *International Journal of Computer Mathematics 92*, 6 (2015), 1204–1221.
11. Kadalbajoo, M. K., and Yadaw, A. S. B-spline collocation method for a two-parameter singularly perturbed convection–diffusion boundary value problems. *Applied Mathematics and Computation 201*, 1-2 (2008), 504–513.
12. Kumari, N., and Gowrisankar, S. A robust b-spline method for two parameter singularly perturbed parabolic differential equations with discontinuous initial condition. *Journal of Applied Mathematics and Computing* (2024), 1–25.
13. Ladyzhenskaia, O. A., Solonnikov, V. A., and Ural'tseva, N. N. *Linear and quasi-linear equations of parabolic type*, vol. 23. American Mathematical Soc., 1968.
14. Linß, T., and Roos, H.- G. Analysis of a finite-difference scheme for a singularly perturbed problem with two small parameters. *Journal of Mathematical Analysis and Applications 289*, 2 (2004), 355–366.
15. Miller, J., O'riordan, E., and Shishkin, G. I. *Fitted numerical methods for singular perturbation problems: error estimates in the maximum norm for linear problems in one and two dimensions*. World scientific, 1996.
16. Miller, J., O'Riordan, E., Shishkin, G. I., and Shishkina, L. Fitted mesh methods for problems with parabolic boundary layers. In *Mathematical Proceedings of the Royal Irish Academy* (1998), JSTOR, pp. 173–190.
17. O'Malley, R. E. Two-parameter singular perturbation problems for second-order equations. *Journal of Mathematics and Mechanics 16*, 10 (1967), 1143–1164.
18. O'Malley, R. E. *Singular perturbation methods for ordinary differential equations*, vol. 89. Springer, 1991.
19. O'Malley, R. E. Introduction to singular perturbations. volume 14. applied mathematics and mechanics. *New York Univ Ny Courant Inst of Mathematical Science* (1974).
20. O'Riordan, E., Pickett, M., and Shishkin, G. I. Parameter-uniform finite difference schemes for singularly perturbed parabolic diffusion-convection-reaction problems. *Mathematics of Computation 75*, 255 (2006), 1135–1154.
21. Roos, H.- G. *Robust numerical methods for singularly perturbed differential equations*. Springer, 2008.
22. Roos, H.- G., and Uzelac, Z. The sdfem for a convection-diffusion problem with two small parameters. *Computational Methods in Applied Mathematics 3*, 3 (2003), 443–458.
23. Shishkin, G. I. The richardson scheme for the singularly perturbed parabolic reaction-diffusion equation in the case of a discontinuous initial condition. *Computational Mathematics and Mathematical Physics 49* (2009), 1348–1368.
24. Shivhare, M., Pramod Chakravarthy, P., and Kumar, D. Quadratic b-spline collocation method for two-parameter singularly perturbed problem on exponentially graded mesh. *International Journal of Computer Mathematics 98*, 12 (2021), 2461–2481.
25. Singh, G., and Natesan, S. Study of the nipg method for two–parameter singular perturbation problems on several layer adapted grids. *Journal of Applied Mathematics and Computing 63*, 1 (2020), 683–705.
26. Vulanović, R. A higher-order scheme for quasilinear boundary value problems with two small parameters. *Computing 67*, 4 (2001).
27. Zahra, W., El- Azab, M., and El Mhlawy, A. M. Spline difference scheme for two-parameter singularly perturbed partial differential equations. *Journal of applied mathematics & informatics 32*, 1_2 (2014), 185–201.

Publisher's Note Springer Nature remains neutral with regard to jurisdictional claims in published maps and institutional affiliations.